

2018-11-13

# Determination and Prediction of Zinc Speciation in Estuaries

Pearson, HBC

<http://hdl.handle.net/10026.1/12860>

---

10.1021/acs.est.8b04372

Environmental Science and Technology

American Chemical Society

---

*All content in PEARL is protected by copyright law. Author manuscripts are made available in accordance with publisher policies. Please cite only the published version using the details provided on the item record or document. In the absence of an open licence (e.g. Creative Commons), permissions for further reuse of content should be sought from the publisher or author.*

1 This is a final revision of manuscript accepted for publication within Environmental  
2 Science and Technology. (<http://dx.doi.org/10.1021/acs.est.8b04372>)  
3

#### 4 **Determination and prediction of zinc speciation in estuaries**

5 Holly B.C. Pearson<sup>a</sup>, Sean D.W. Comber<sup>a\*</sup>, Charlotte B Braungardt<sup>a</sup>, Paul Worsfold<sup>a</sup>,  
6 Anthony Stockdale<sup>b</sup> and Stephen Lofts<sup>c</sup>

7 <sup>a</sup> School of Geography, Earth and Environmental Sciences, University of Plymouth,  
8 Plymouth Devon, PL4 8AA, UK.

9 <sup>b</sup> School of Earth and Environment, University of Leeds, LS2 9JT, UK.

10 <sup>c</sup> Centre for Ecology & Hydrology, Lancaster Environment Centre, Library Avenue,  
11 Bailrigg, Lancaster, LA1 4AP, UK.

12  
13 \* Corresponding author: [sean.comber@plymouth.ac.uk](mailto:sean.comber@plymouth.ac.uk)  
14

#### 15 **Abstract**

16 Lowering of the estuarine Environmental Quality Standard for zinc in the UK to 121 nM  
17 reflects rising concern regarding zinc in ecosystems and is driving the need to better  
18 understand its fate and behaviour and to develop and parameterise speciation models to  
19 predict the metal species present. For the first time, an extensive dataset has been gathered  
20 for the speciation of zinc within an estuarine system with supporting physico-chemical  
21 characterization, in particular dissolved organic carbon. WHAM/Model VII and Visual  
22 MINTEQA2 speciation models were used to simulate zinc speciation, using a combination of  
23 measured complexation variables and available defaults. Data for the five estuarine  
24 transects from freshwater to seawater endmembers showed very variable patterns of zinc  
25 speciation depending on river flows, seasons, and potential variations in metal and ligand  
26 inputs from *in situ* and *ex situ* sources. There were no clear relationships between free zinc  
27 ion concentration [Zn<sup>2+</sup>] and measured variables such as DOC concentration, humic and  
28 biological indices. Simulations of [Zn<sup>2+</sup>] carried out with both models at high salinities or by  
29 inputting site specific complexation capacities were successful, but overestimated [Zn<sup>2+</sup>] in  
30 low salinity waters, probably owing to an underestimation of the complexation strength of the  
31 ligands present. Uncertainties in predicted [Zn<sup>2+</sup>] are consistently smaller than standard  
32 deviations of the measured values, suggesting that the accuracy of the measurements is  
33 more critical than model uncertainty in evaluating the predictions.  
34

35 **Keywords: Zinc, speciation, estuary, WHAM, model, Visual MINTEQ**

## 36 **1. Introduction**

37 Zinc (Zn) is ubiquitous in the aquatic environment and, whilst an essential element for all  
38 organisms, can be toxic in excess. In 2013 the UK Environmental Quality Standards (EQS)  
39 for Zn in saline waters was lowered from 612 nM ( $40 \mu\text{g L}^{-1}$ ) to 121 nM ( $7.9 \mu\text{g L}^{-1}$ , including a  
40  $17 \text{ nM}$  ( $1 \mu\text{g L}^{-1}$ ) allowance for background concentrations) dissolved metal. Such a revision  
41 reflects the awareness that Zn is a potential pollutant, yet there has been a paucity of data  
42 published on its speciation in estuarine and coastal waters, particularly regarding the free  
43 metal ion concentration.<sup>1</sup> The reasons for this are related to low concentrations (relative to  
44 freshwaters) present in estuarine and coastal waters, relatively weak complexation of Zn with  
45 dissolved organic ligands and a saline matrix, leading to significant analytical challenges.<sup>2</sup>

46 EQS have been set or proposed for a number of trace elements including Cu, Ni and Zn in  
47 freshwaters taking account of the bioavailability of metals by using either Biotic Ligand Models  
48 (BLMs) or statistical models by using factors such as pH, calcium and dissolved organic  
49 carbon (DOC).<sup>3-6</sup> In estuarine and coastal waters, however, the development of BLM has been  
50 more challenging owing to the complex matrix and the constantly changing physico-chemical  
51 characteristics, such as salinity, suspended solids and organics (both natural and  
52 anthropogenic). Recently, a BLM approach been proposed for Cu in saline waters by the US  
53 EPA<sup>7</sup> based on USEPA 2007 information,<sup>3</sup> but no BLM or BLM-influenced statistical model  
54 approach as of yet has been developed for Zn in salt waters.

55 The ability to predict the free metal ion concentration is pre-requisite to setting a scientifically  
56 robust EQS that takes metal speciation into account. Thermodynamic equilibrium models have  
57 been developed (e.g. WHAM/Model VII,<sup>8,9</sup> FIAM<sup>10</sup> and Visual MINTEQ<sup>11</sup>) for calculating the  
58 speciation of trace elements in fresh waters and these can also be applied to saline waters  
59 successfully.<sup>1</sup> However, in many cases there are fewer data available for validating model  
60 outputs particularly complexing ligand concentrations and strength. A recent review showed  
61 that, since 1984, only four papers reported  $[\text{Zn}^{2+}]$  in estuaries across the USA, Netherlands  
62 and SE Asia<sup>2</sup> and not all of them covered the full salinity range expected in an estuary.

63 Five surveys carried out on a temperate flooded river valley estuary in the SW of England  
64 (Tamar) have generated comprehensive Zn speciation data, including free metal ion  
65 concentrations, complexation capacity and natural ligand dissociation constants, using  
66 competitive ligand exchange cathodic stripping voltammetry (CLE-AdCSV).<sup>2</sup>

67 The aim of this study was to provide essential information required for the development of an  
68 estuarine BLM for Zn. To this end, the Zn speciation within the Tamar estuary was appraised

69 against physico-chemical parameters, such as salinity and DOC, and the latter was  
70 characterized further using fluorimetric analysis<sup>12,13</sup> of the organic components present.  
71 Furthermore, the predictive ability of WHAM VII and Visual MINTEQ<sup>14</sup> for Zn speciation was  
72 tested and compared. The combination of Zn speciation determination and modeling  
73 presented here represents a stepping stone to more effective regulation of this metal within  
74 saline environments.

75

## 76 **2. Methods**

### 77 **2.1 Tamar catchment and sampling sites**

78 The Tamar estuary (16 km in length) runs from Gunnislake Weir to the English Channel and  
79 comprises two significant tributaries of the Lynher and Tavy (Figure S1).<sup>15</sup> The estuary has  
80 been contaminated with metals from a variety of sources including previous mining of arsenic,  
81 copper, zinc and lead;<sup>16</sup> from the dockyards and marinas using zinc anodes and antifoulant  
82 paints;<sup>17</sup> and effluents from sewage works containing metals as well as potentially complexing  
83 ligands (Figure S1).<sup>18</sup> Other sources of metal complexing ligands include spring and summer,  
84 phytoplankton blooms in the lower estuary as observed via chlorophyll 'a' measurement in this  
85 work (Figure S2) and previously.<sup>19</sup> Five full estuary transects (typically 8 sampling stations)  
86 were undertaken between July 2013 and February 2013 covering different seasons with  
87 variations in river flow, salinity, and the presence of phytoplankton blooms during the spring  
88 and summer months. Not all surveys have a complete data set owing to practicalities and  
89 sampling based on trying to achieve a representative range of salinities, which is reflected in  
90 the representation of surveys in some graphs and tables.

### 91 **2.2 Chemicals and reagents**

92 As previously reported<sup>20</sup> all chemicals used were of analytical grade or higher and ultrahigh  
93 purity (UHP) water (Elga Process Water, resistivity = 18.2 MΩ cm) and trace metal  
94 specification hydrochloric acid (6 M, ROMIL SpA) was used throughout to minimise  
95 contamination from Zn. Zn standards were prepared from Romil PrimAg reference solutions.  
96 All samples were buffered (pH 7.8 (+/- 0.1)) using HEPES buffer (1 M) prepared from N-  
97 hydroxyethylpiperazine-N'-2'-ethanesulphonic acid (Biochemical grade, BDH Laboratory  
98 Supplies). The competitive ligand; ammonium pyrrolidine dithiocarbamate (APDC; Fisher  
99 Scientific) was made up as a stock 1 M solution prior to dilution to 40 and 4 μM for  
100 complexation capacity titrations. Samples for total dissolved Zn concentration ( $[Zn_{TD}]$ ) were  
101 acidified with hydrochloric acid (6 M, ROMIL SpA).

### 102 **2.3 Sampling protocol**

103 Section S1 (ESI) details the sampling protocol. Prior to use, all sampling and filtration  
104 equipment was acid washed (10% HCl) and rinsed with UHP water. Water samples for metal  
105 speciation were filtered through 0.4  $\mu\text{m}$  polycarbonate membranes (Whatman Nuclepore  
106 Track-Etched) onsite and frozen at  $-20^{\circ}\text{C}$  in low density polyethylene bottles (Nalgene) prior  
107 to analysis.  $[\text{Zn}_{\text{TOD}}]$  samples were refrigerated and determined within 48 h at room temperature.  
108 Samples for DOC were filtered (0.7  $\mu\text{m}$  GF/F) within 24 h of collection, acidified to ca. pH 2,  
109 and refrigerated in glass vials.

### 110 **2.4 Analytical methods, procedures and calculations**

111 All dissolved Zn analysis was undertaken by CLE-AdCSV (Section S2).

#### 112 **2.4.1 Total dissolved Zn**

113 Prior to  $[\text{Zn}_{\text{TOD}}]$  determinations, acidified samples were UV irradiated after the addition of  
114 hydrogen peroxide (final concentration of 15 mM). Sample pH was adjusted to ca. 6 with  
115 ammonia solution (SpA, ROMIL) prior to addition of the HEPES buffer and APDC for  
116 determination using voltammetry described in section S2. Certified reference materials  
117 (CRMs) were used for every batch of samples. Recoveries were between 90 and 109%,  
118 with a typical precision of  $\leq 10\%$  RSD. The limit of detection (LOD) was typically 0.33 nM Zn  
119 under optimum conditions. (maximum drop size, stirring speed and 60 s deposition time).

#### 120 **2.4.2 Free Zn ion, complexation capacity and conditional stability constants**

121 Complexation capacity titrations (CCT) were performed using the same procedures as  
122 described elsewhere.<sup>20</sup> Briefly, titrations (at pH 7.8 using HEPES buffer) were carried out  
123 at two competitive ligand strengths (4 and 40  $\mu\text{M}$  APDC) providing detection windows of  
124  $\log \alpha_{\text{ZnAPDC}} = 3.01 - 4.59$  and  $3.03 - 5.29$ , respectively, matching that expected for  
125 estuarine samples. A total of 10 Zn additions were performed on duplicate samples, with  
126 overnight equilibration. Each sample aliquot was determined in triplicate by CLE-AdCSV  
127 using analytical parameters provided in Section S2. Data were transformed using a  
128 method reported by van den Berg/Ruzic<sup>21,22</sup> to quantify the sample ligand concentration  
129  $[\text{L}_x]$  (in nM), the conditional stability constant of the Zn-natural ligand complexes  
130 ( $\log K'_{\text{ZnL}_x}$ ) and  $[\text{Zn}^{2+}]$ , with data reported as nM or  $\text{pZn}^{2+}$  (the negative logarithm of the  
131 Zn concentration, rather than activity).

132

133 High temperature catalytic combustion (Shimadzu TOC V analyser)<sup>23</sup> was used to determine  
134 Dissolved Organic Carbon (DOC) with appropriate certified reference materials<sup>20</sup> providing a  
135 limit of detection of 4  $\mu\text{M}$ . Characterisation of the DOC was carried out using 3-D fluorimetry  
136 with a Hitachi F-4500 FL spectrophotometer. Sigma Aldrich humic acid (55.1% C; Sigma

137 Aldrich, UK) and Nordic aquatic fulvic acid reference material supplied by the International  
138 Humic Substances Society (45% C) were used as standards. Although the limitations of using  
139 commercial humic acids have been reported,<sup>24</sup> the Sigma Aldrich material is well characterized,  
140 available and being terrestrially derived, matched the likely sources of humic material likely to  
141 be present in the Tamar catchment and so was considered fit for purpose.

## 142 **2.5 Thermodynamic equilibrium speciation calculations**

### 143 **2.5.1 Visual MINTEQ**

144 Calculations were undertaken using the Visual MINTEQ (VM) version 3.1,<sup>14</sup> chemical  
145 equilibrium model for the calculation of metal speciation, solubility equilibria, sorption etc. for  
146 natural waters. It offers the benefit of a Windows interface and the ability to introduce new  
147 ligands (in this case  $\log K'_{ZnL_x}$  values and ligand concentrations derived from the CCT field  
148 data at two separate artificial ligand strengths) into its database. Input major cation and anion  
149 concentrations were generated from determined parameters (salinity, pH) using an ion-pairing  
150 model.<sup>25</sup>

151  $[Zn^{2+}]$  predictions were generated using the following input parameters (further default  
152 parameters in Table S3):

- 153 1) Major ion concentrations were predicted from assumed conservative mixing of Tamar  
154 freshwater (mean concentrations from Gunnislake sample from present surveys and  
155 available Environment Agency data) and sea water<sup>26</sup> end member data obtained from  
156 an ion-pairing seawater model (Table S3).
- 157 2)  $[Zn_{TD}]$  determined as part of this work.
- 158 3) Ligand concentrations:
  - 159 a. Taken from this work using 4 and 40  $\mu$ M APDC with their accompanying  
160 conditional stability constants.
  - 161 b. Ligands predicted by VM 3.1 using measured DOC concentrations from this  
162 study combined with the SHM, Gaussian and Nica-Donnan model options (see  
163 section S3).

164 All modeling was carried out assuming a pH 7.8 to match the conditions under which the  
165 experimental work was carried out and at a fixed temperature of 15 °C. The Davies method  
166 was used for activity correction, without other organic ligands present at an assumed  
167 thermodynamic equilibrium. Sensitivity analyses (not shown reported) for temperature and pH  
168 within VM using natural sample values showed negligible difference in predicted  $[Zn^{2+}]$ .

### 169 **2.5.2 WHAM/Model VII**

170 WHAM/Model VII was used to predict Zn speciation under the assumption that the dissolved  
171 organic matter (DOM) in the estuarine water behaves in the same way as if composed of soil

172 and freshwater fulvic and humic acid extracts in competition with inorganic ligands. WHAM VII  
173 comprises two components, the inorganic speciation code WHAM<sup>8</sup> and Humic Ion Binding  
174 Model VII, described in detail in elsewhere.<sup>9</sup>

175 To run the model, the pH used for the laboratory Zn speciation measurements and determined  
176 Zn concentrations were applied. Major ion concentrations (except carbonate) were obtained  
177 using a combination of salinity and freshwater endmember major ion measurements. Modeling  
178 was done under two scenarios of differing carbon dioxide equilibration between the  
179 atmosphere and water. In Scenario S1, carbonate speciation was determined using the default  
180 equilibria and binding constants, assuming equilibrium with the atmosphere and a partial  
181 pressure of CO<sub>2</sub> of 400 ppm. In Scenario S2, in order to maintain consistency with typical  
182 methods for evaluating the carbonate system in marine environments, [CO<sub>3</sub><sup>2-</sup>] was calculated  
183 using the CO2SYS model<sup>27</sup> with the constants describing the carbonate and sulphate  
184 equilibrium with hydrogen ions<sup>28</sup> and refitted as described elsewhere<sup>29,30</sup> respectively. The pH  
185 was on the total scale and the total boron concentration from Uppström, (1974). This approach  
186 was used recently,<sup>31</sup> implementing the carbonate system with measured conditional stability  
187 constants into Visual MINTEQ. Detailed information regarding WHAM VII in section S4.

188 Uncertainty in predictions was modelled using repeated estimates of input measurements and  
189 model parameters made using the assumption of a normal or log-normal distribution around  
190 the measured or default value, coupled with an absolute or relative error value.<sup>32</sup> Here  
191 previously reported error values were applied of: ±0.1 absolute error on measured pH, ±5%  
192 relative error on measurements except for DOC, ±9% relative error on DOC, ±1K absolute  
193 error on temperature, and ±0.3 absolute error on the intrinsic metal-fulvic binding constant.<sup>32</sup>  
194 The number of repeat calculations was 2000 and uncertainties were computed as the 15.9<sup>th</sup>  
195 and 84.1<sup>th</sup> percentiles of the population of predicted free ion concentrations. This range of  
196 percentiles corresponds to ±1 standard deviations from the mean for a normally distributed  
197 dataset.

198

199

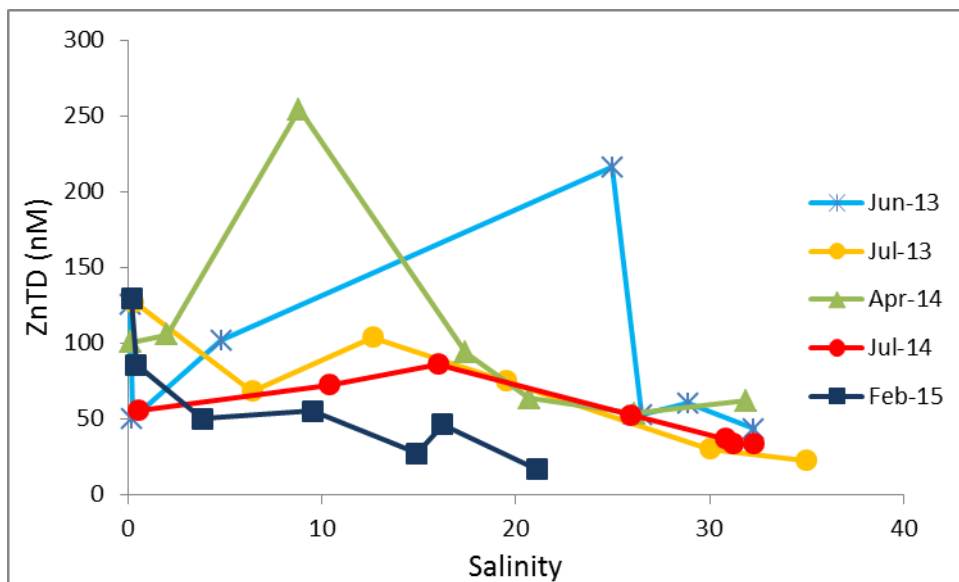
200

201 **3. Results and Discussion**

202

203 **3.1. Total dissolved zinc**

204 In the Tamar estuary,  $[Zn_{TD}]$  ranged from 11 - 225 nM, with typically, highest concentrations  
 205 observed at the historically mine-influenced freshwater end member (FWEM) (Figure 1). The  
 206 non-conservative mixing profiles (Figure 1) show removal of Zn at the freshwater-seawater  
 207 interface (FSI) for all the surveys, and further reduction of Zn concentrations toward the  
 208 seawater end member (SWEM). Even with the observed non-conservative behaviour of  $Zn_{TD}$   
 209 and dilution with seawater within the estuary, there were some exceedances of the new EQS  
 210 (104 nM). This was particularly noticeable within the mid-estuarine area, where distinct inputs  
 211 of Zn were observed during the July 2013 and April 2014 surveys. These inputs were the likely  
 212 result of Zn desorption from sediment, resuspended by tidal forces from an expanse of mud  
 213 flats extending from the road bridge at Saltash to Pentillie Castle (typical salinity 10 to 15),  
 214 where the estuary channel narrows. Kinetic experiments conducted by previously<sup>33</sup>  
 215 demonstrated a pulse of Zn released from sediments (estuarine and riverine) within 10 min of  
 216 its exposure to seawater, and attributed mid-estuarine dissolved Zn maxima partially to  
 217 desorption. Therefore, the peak in dissolved Zn observed at Pentillie Castle during the April  
 218 survey and at Halton Quay during July 2013 may be explained by desorption, combined with  
 219 tidally induced porewater infusions.



220

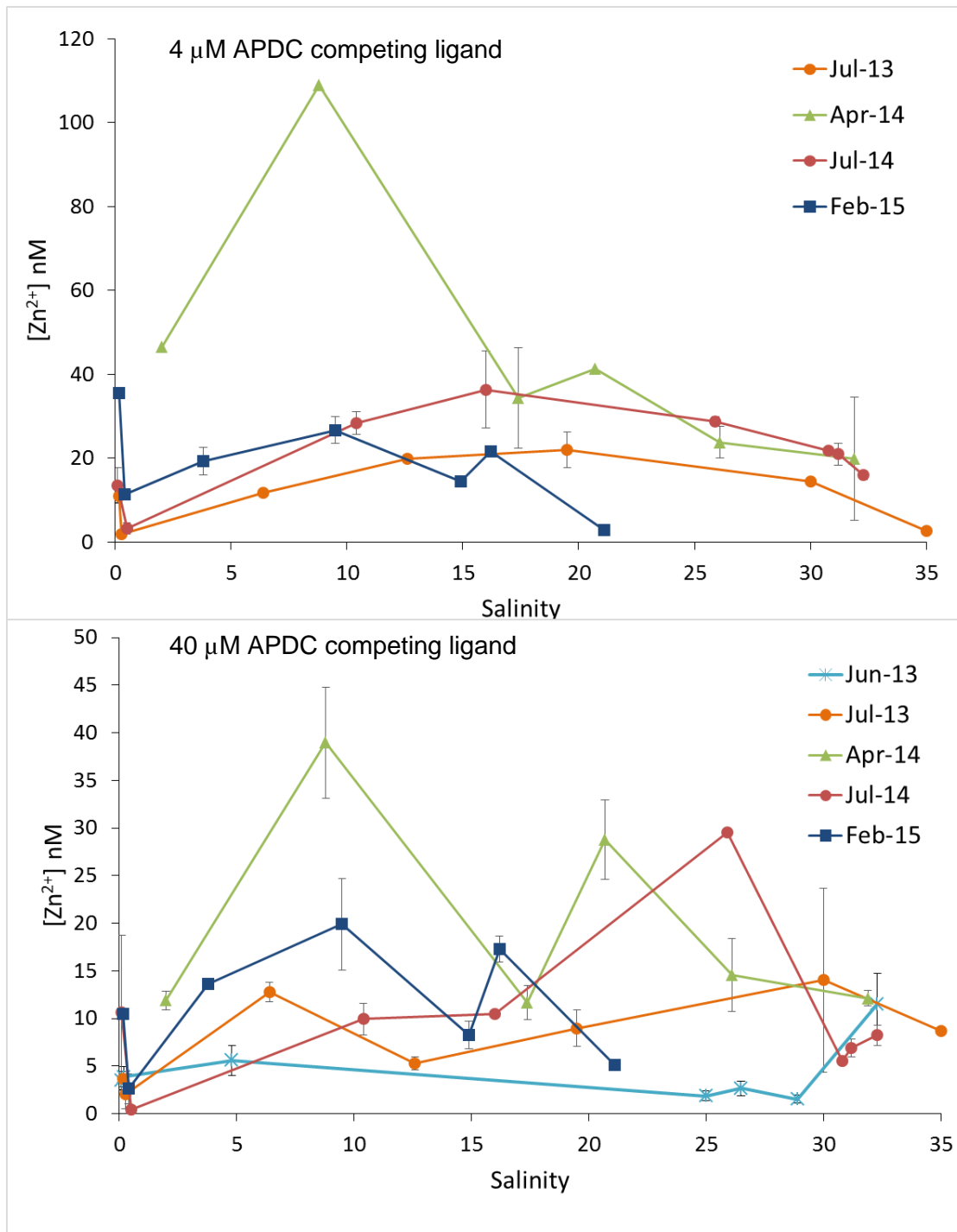
221 **Figure 1. Total dissolved Zn concentrations determined for the four transects. Note: In**  
 222 **April 2015, a sample was taken at low salinity within the estuary, but logistical**  
 223 **constraints prevented the sampling of a fresh water endmember in the river.**

224

225 **3.2. Zinc speciation and ligand characteristics**

226 Concentrations of  $Zn^{2+}$ , determined using the two competing ligand strengths, ranged from 0.3  
227 – 109 nM (Figure 2) whereby the lowest range of concentrations occurred in July 2013 and  
228 the highest in April 2014. These concentrations are of the same order as the very limited data  
229 for  $[Zn^{2+}]$  provided in literature.<sup>34</sup> The fresh and seawater endmembers contained the lowest  
230  $[Zn^{2+}]$  and during all surveys concentrations increased at some location between these two  
231 endmembers. Although the trends are broadly similar, results from determinations with the  
232 weaker competitive ligand strength (4  $\mu$ M APDC) returned higher  $[Zn^{2+}]$  than determinations  
233 using 40  $\mu$ M APDC. This is a clear indication that differences in the analytical detection window  
234 introduce bias into the determination of  $[Zn^{2+}]$ .

235 Notwithstanding this artefact, in terms of toxicity,  $[Zn^{2+}]$  determined in this study are potentially  
236 harmful to sensitive aquatic organisms along the whole of the estuary, even at the lower  $[Zn^{2+}]$   
237 concentrations determined with 40  $\mu$ M APDC. For example, the growth rate of marine  
238 phytoplankton *Synechococcus* sp. has been reported to decline at concentrations of  $[Zn^{2+}] >$   
239 0.4 nM and this value is  $[Zn^{2+}] > 3.2$  nM for *Thalassiosira weissflogii*.<sup>35</sup>



240

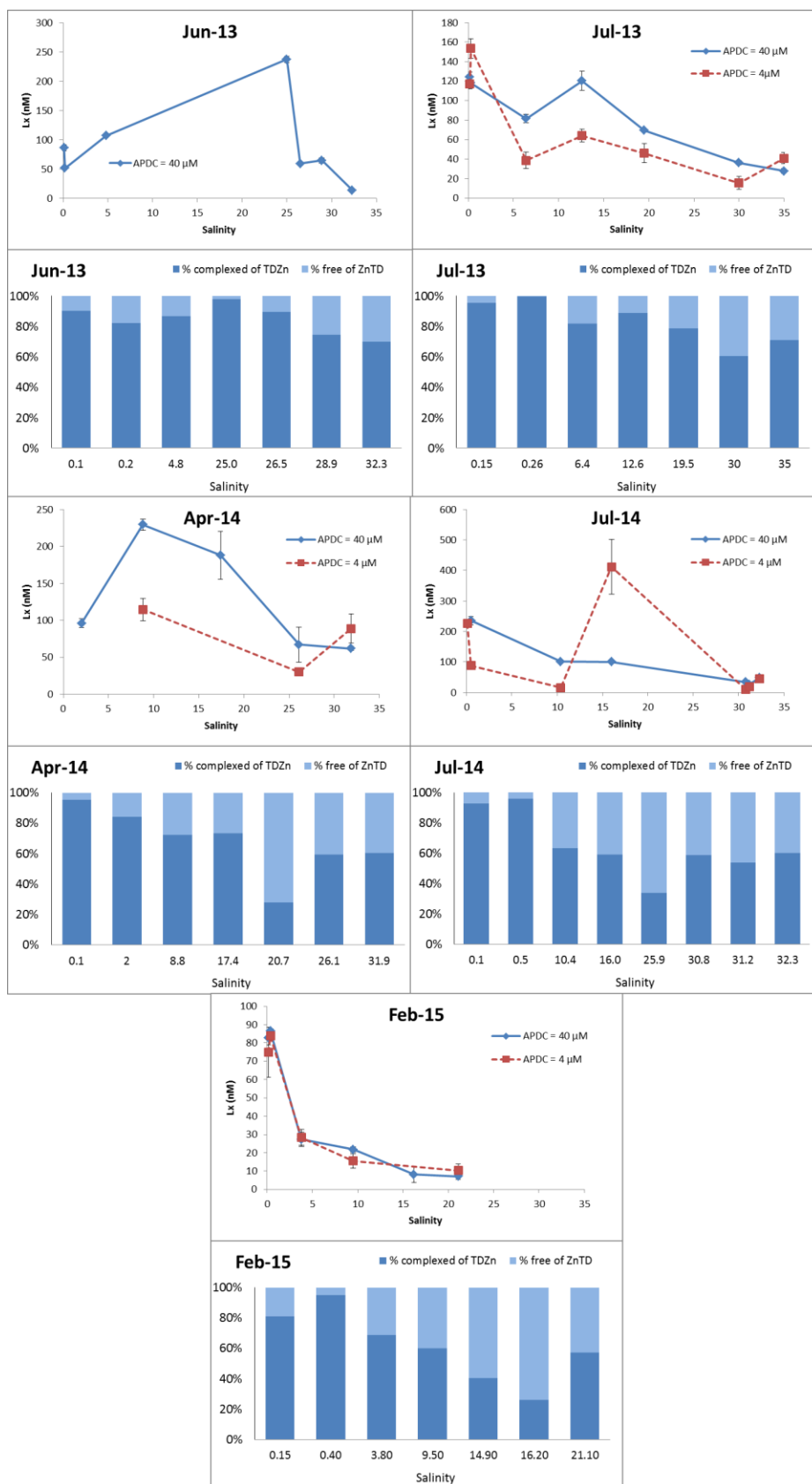
241 **Figure 2. Free Zn concentrations ( $[Zn^{2+}]$  determined using various concentrations of**  
 242 **APDC) plotted as a function of salinity for the Tamar transects. Each data**  
 243 **point is the average of two duplicate analyses (one on each filter fraction) with**  
 244 **error bars representing the range. Where error bars are absent, only one data**  
 245 **point was obtained. Nb. There was no determination of  $[Zn^{2+}]$  for the Jun-13**  
 246 **survey for 4  $\mu$ M competing APDC ligand**

247

248 In general, the percentage of  $[Zn^{2+}]$  as a fraction of the  $[Zn_{TD}]$  increased with salinity for both  
 249 ligand strengths (4 and 40  $\mu$ M APDC) used to determine complexation capacity by Zn titration

250 (Figure 3), and, to a degree, reflects the observed Lx:Zn<sub>TD</sub> ratio (Figure S3). Increasing salinity  
251 introduces high cation (e.g. calcium, magnesium) concentrations that compete with Zn  
252 complexing sites on ligands, therefore raising the potential for more Zn to be less strongly  
253 complexed.

254 Concentrations of zinc complexing ligands ([Lx]) between 3 and 412 nM were determined  
255 (Figure 3), well within the range reported for other estuarine and coastal studies (5 – 220  
256 nM).<sup>34,36</sup> Although some inputs of Zn ligands mid-estuary were apparent in June 2013, April  
257 2014 and to some extent July 2014, the highest concentrations, and hence main inputs, were  
258 at the FWEM. Zn ligand concentrations, in most cases, tracked the total dissolved metal  
259 concentration profiles with salinity, indicating that both the FWEM and tidally induced mid-  
260 estuarine sediment processes were sources for Zn<sub>TD</sub> and Lx (Figures 1 and 3). The degree of  
261 Zn complexation varied between detection windows, with higher proportions of [Zn<sup>2+</sup>] present  
262 at the weaker analytical competition strength. Variation between surveys was also apparent.  
263 In February 2015 the proportion of [Zn<sup>2+</sup>] in samples was high (32 – 49 %) in the mid- and  
264 lower estuary, even though Zn<sub>TD</sub> concentrations were similar to those during other surveys.  
265 This reflects the low complexation capacity determined at both APDC concentrations, lack of  
266 ligand excess (Figure S3) and low DOC concentrations (31 – 123 µm C) observed during this  
267 survey (Table S2).



268

269  
270  
271  
272

**Figure 3. Ligand concentrations ([Lx]) and proportion of Zn complexed (organically) versus proportion free Zn<sup>2+</sup> ion as a percentage of total dissolved Zn for each sampling occasion. The x-axes represent salinity in all cases. Error bars on [Lx] plots represent ± an average uncertainty.**

273

274 The ratio  $[Lx]:[Zn_{TD}]$  indicates the significance of  $Zn^{2+}$  present in the water, whereby  $[Lx]:[Zn_{TD}] >$   
275 1 signifies an excess of Zn complexing ligands and therefore suppression of the more  
276 bioavailable and toxic  $Zn^{2+}$  species. Saturation of ligands is indicated by  $[Lx]:[Zn_{TD}] < 1$ , with  
277  $[Zn^{2+}]$  likely to be more prevalent as the ratio decreases. The ratio showed no relation to salinity  
278 in any of the surveys.  $[Lx]:[Zn_{TD}]$  was consistently low (average 0.5) in February 2015 - only  
279 at Cotehele ( $S = 0.4$ ) did it approach 1 (Figure S3), a profile that indicates ligand saturation  
280 throughout the estuary, concomitant with the high proportion of  $Zn^{2+}$  observed. In June and  
281 July 2013 and April 2014, ratios between 0.4 and 2.1 indicated varied profiles with most  
282 samples exhibiting little excess ligand. In July 2014, ratios varied between 0.2 and 4.8, with  
283 highest values at Morwellham (4.2,  $S=0.5$ ) and Cotehele (4.8,  $S=16$ ), where observed ligand  
284 concentrations far outweighed the presence of  $Zn_{TD}$ . Overall, complexing capacity is exceeded  
285 (ratio  $< 1$ ) in 30 of the 53 measurements depending on titration competition strength and time  
286 of year, which explains the occurrence of  $[Zn^{2+}]$  in the samples.

287

### 288 **3.3 Prediction of $[Zn^{2+}]$ in estuarine waters**

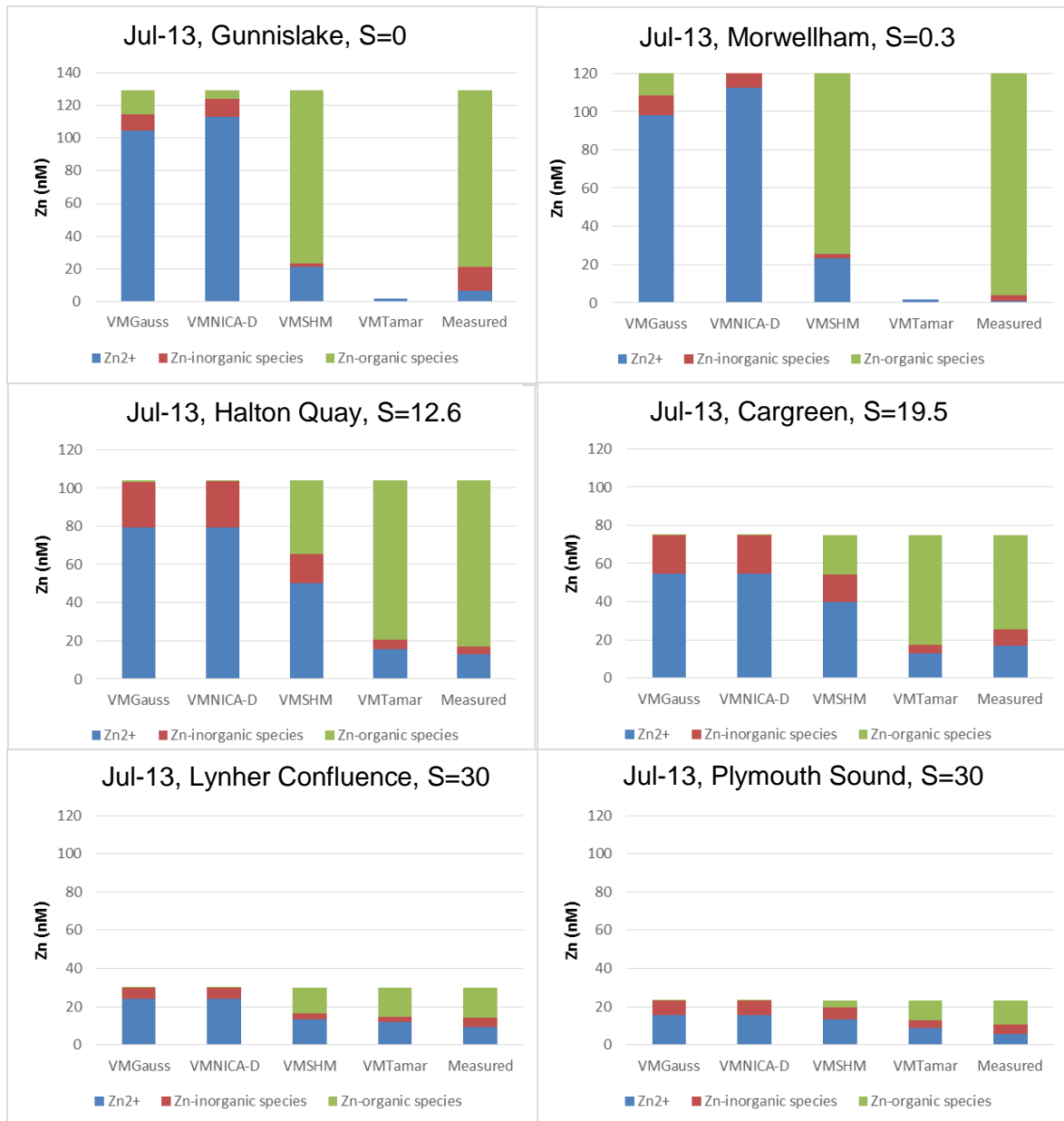
289 Measuring  $[Zn^{2+}]$  within any given estuary provides an indication of possible bioavailable  
290 concentrations. However, to develop a BLM or to be able to extrapolate data to other estuaries  
291 then the ability to accurately predict the Zn speciation is essential.

292 Figure 4 provides a detailed analysis of VM outputs using the input parameters detailed in the  
293 methodology section and Table S3 of the ESI. VM provides three options for converting DOC  
294 concentrations to metal complexing ligands, the Nica-Donnan, Gaussian and Stockholm  
295 Humic Models). The theory associated with these calculations is provided in S3 of the ESI.  
296 For six sites of varying salinity from 0 to 33 where a full dataset was available, the model was  
297 run using the three options for predicting metal complexation based on inputted DOC  
298 concentration (Gaussian, Nica Donnan and Stockholm Humic Model).

299

300

301



302

303

304

305

306

307

**Figure 4. Comparison of measured and predicted Zn speciation (free ion, inorganic and organic) using the ligand predicting models within Visual MINTEQ (VM). VMGauss = Gaussian model; VMNICA-D = Nica-Donnan model; VMSHM = Stockholm Humic Model; VM Tamar = VM inputs of measured ligand strength and concentration for July 2013 samples in the Tamar estuary from a range of salinities (except 0 and 2.3).**

308

309

310

311

312

313

The distribution of Zn between free ion, inorganic and organically complexed species varied considerably among the different approaches to estimating complexing ligand strength and concentrations. When site-specific measured complexation capacity and ligand concentration were entered into VM, the best fit between measured and calculated Zn<sup>2+</sup> and organically bound Zn was achieved (Figure 5 and S3). Where only DOC concentration was entered and VM was used to predict Zn complexation using the three options available, [Zn<sup>2+</sup>] was

314 overestimated in all samples, compared to measured values. At low to moderate salinities the  
315 Gaussian and Nica-Donnan methods significantly overestimated  $[\text{Zn}^{2+}]$ , and consequently  
316 underestimated the organically-bound Zn. The Stockholm Humic Model (VMSHM) offers a  
317 much closer agreement. At higher salinity, total dissolved concentrations and Zn complexing  
318 ligands present in the samples were lower, and consequently the fraction of  $\text{Zn}^{2+}$  increased  
319 (Figure 3). The pattern between the different methods of calculating Zn complexation remains  
320 the same with only the VMSHM approach predicting significant organic ligand complexation  
321 and hence, corresponding reductions in  $[\text{Zn}^{2+}]$ .

322 For the WHAM/Model VII, Scenario S2 generates a significantly greater quantity of  $\text{ZnCO}_3$  and  
323  $\text{ZnHCO}_3^+$ , and average of  $21.4 \pm 4$  nM SD and  $21.5 \pm 4$  nM SD ( $n = 44$ ), respectively. This has  
324 the effect of significantly reducing  $[\text{Zn}^{2+}]$  and bringing it more in line with the measured values  
325 using voltammetry (Figures 5 and S4).

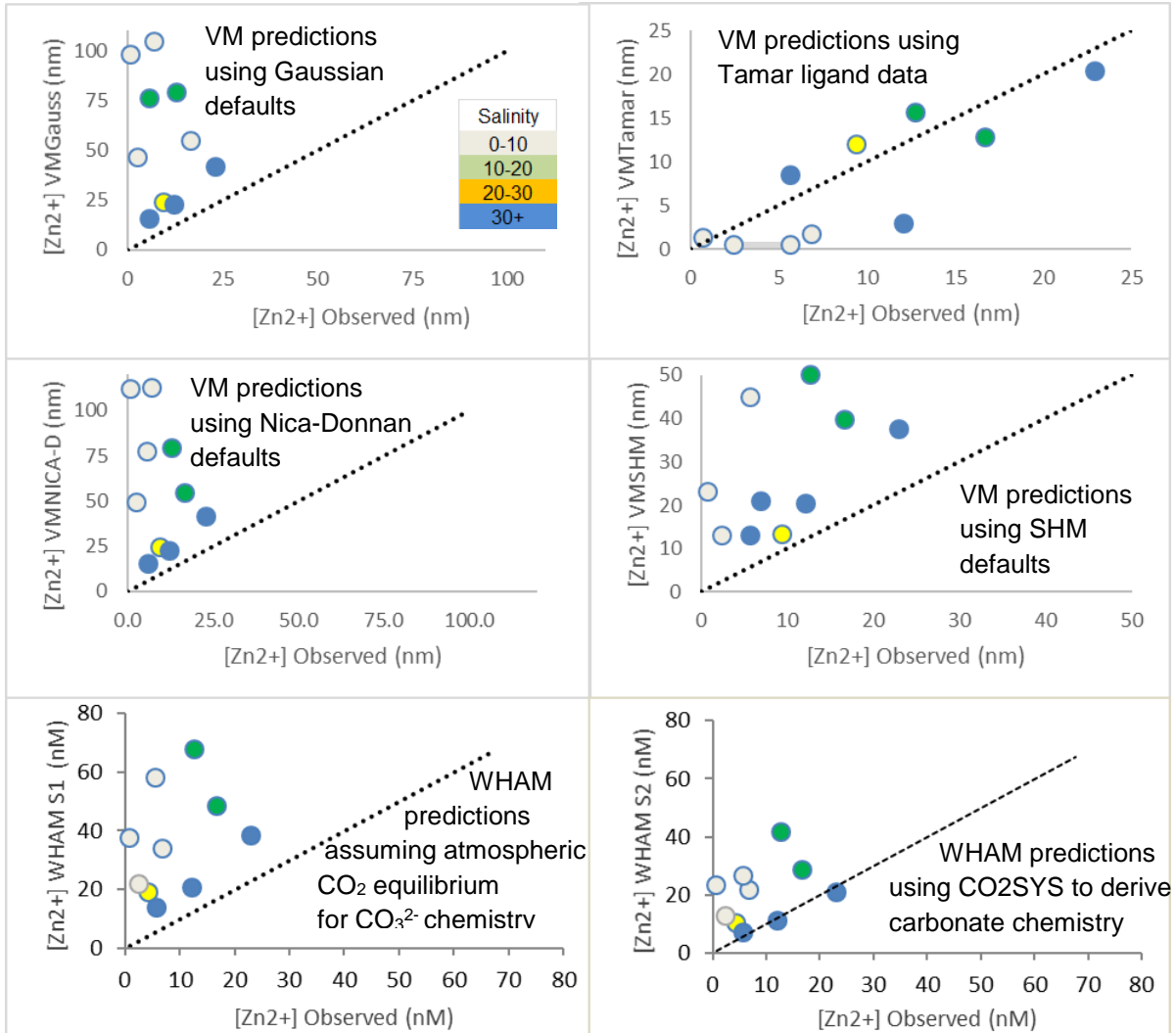
326

327

328

329

330



331

332 **Figure 5. Predicted versus measured  $Zn^{2+}$  concentrations (nM) using the VM and**  
 333 **WHAM/ModelVII models.**

334

335 The data points representing the largest discrepancy in  $[Zn^{2+}]$  (the most over- or under-  
336 predicted by the model) between predicted and measured values are for samples located at  
337 low salinity zones ( $< 1$ ) in the upper estuary (Gunnislake, two samples from Morwellham Quay,  
338 Cotehele, Figure 5) for both, VM and WHAM. In these locations, humic and fulvic type ligands  
339 were dominant (see below) and present at relatively high concentrations. Measured log  $K$   
340 values for Zn-organic complexes at these sites ranged between 7.74 and 9.66, which is much  
341 higher than, for example, the assumption used for the  $VM_{NICA-D}$  calculations.  $VM_{NICAD-D}$   
342 assumes complexation by fulvic acid alone (log  $K = -3.84$  for carboxylic and log  $K = 0.73$  for  
343 phenolic functional groups, respectively).

344 The measured log  $K$ s are conditional binding constants, which are specific to the water  
345 composition, as they do not consider the influence of competition for binding to organic matter  
346 – particularly competition from the  $H^+$  ion. The log  $K$ s in the models (at least in WHAM and the  
347 SHM) are thermodynamic constants for the binding of the metal to a single binding site on a  
348 humic molecule. Competition is provided by having similar constants for other cations  
349 (including  $H^+$ ). More importantly from the point of view of the apparent binding strength, in  
350 WHAM and the SHM pairs and triplets of single binding sites can form bidentate and tridentate  
351 sites, respectively. These have log  $K$ s that are the sum of the log  $K$ s for the sites that make  
352 them up and thus have higher metal binding affinities, closer to those of the ligands identified  
353 by measurement. The better agreement between observed and computed  $Zn^{2+}$  when using  
354 the measured ligand concentrations is due to the fact that there is a strong element of fitting  
355 involved, i.e. the initial determination of ligand concentration and binding strength. It ought to  
356 be equally possible to fit any of the other models to the titration data and obtain improved  
357 agreement with the field data.

358 As with the SHM, NICA–Donnan and Gaussian models, assumptions regarding the humic  
359 composition of DOC are required to perform computations in WHAM if only DOC concentration  
360 is available as a measure of the organic matter. In past applications of WHAM this has been  
361 done by assuming a proportion of the DOC to behave as model fulvic acid (FA) and the  
362 remainder to be inert with respect to ion binding. Lofts and Tipping<sup>32</sup> computed a mean DOC  
363 to “active” FA ratio of 1.27, based on previous work.<sup>37</sup> However, the ratios obtained by Bryan  
364 and co-workers<sup>37</sup> from 14 freshwaters showed an inter sample variation by a factor of over  
365 two, from 0.80 to 1.82. Results demonstrate the importance of using an appropriate approach  
366 for handling carbonate speciation and show predictions for marine systems are improved with  
367 this approach. Furthermore, if there were more comprehensive data on the nature of marine  
368 DOM and transitions across salinity gradients these could be built into generic models.  
369 However, the (current) reliance on freshwater and soil fulvic acid/humic acid data means some  
370 discrepancy is likely if the two end member DOMs are different in character (see Section 3.5).

371 Whilst this research shows reasonable predictions can be achieved for estuarine/seawater, it  
372 has been shown that as the waters get more saline the trend is for a greater discrepancy  
373 between measurement and modeling.<sup>38</sup>

374 Uncertainties for WHAM VII predictions are shown in Figure S6. Predictions include estimates  
375 of uncertainty due to uncertainty in measurements and parameters, using the Monte Carlo  
376 approach.<sup>9</sup> The prediction uncertainties cover the 15.9–84.1 percentile range of model outputs,  
377 equivalent to  $\pm 1$  standard deviation. Patterns of goodness-of-prediction against salinity are  
378 generally similar to those for the other models. Measurements in samples of salinity  $\geq 30\text{‰}$   
379 ( $n = 4$ ) are reproduced well by the modeling, with all predictions within the  $\pm 1$  standard  
380 deviation range of measurement. In salinities of 1–30‰ ( $n = 3$ ), predictions are reasonable.  
381 Predictions in samples of salinity  $\leq 1\text{‰}$  underestimate of the observed extent of Zn  
382 complexation. Uncertainties in predicted  $[\text{Zn}^{2+}]$  are consistently smaller than standard  
383 deviations of the measured values, suggesting that the accuracy of the measurements is more  
384 critical than model uncertainty in evaluating the predictions.

385 An important observation is that in terms of potentially using these models for implementing  
386 an EQS, that none of the default modes lead to over-prediction of measurements and therefore  
387 will be conservatively protective.

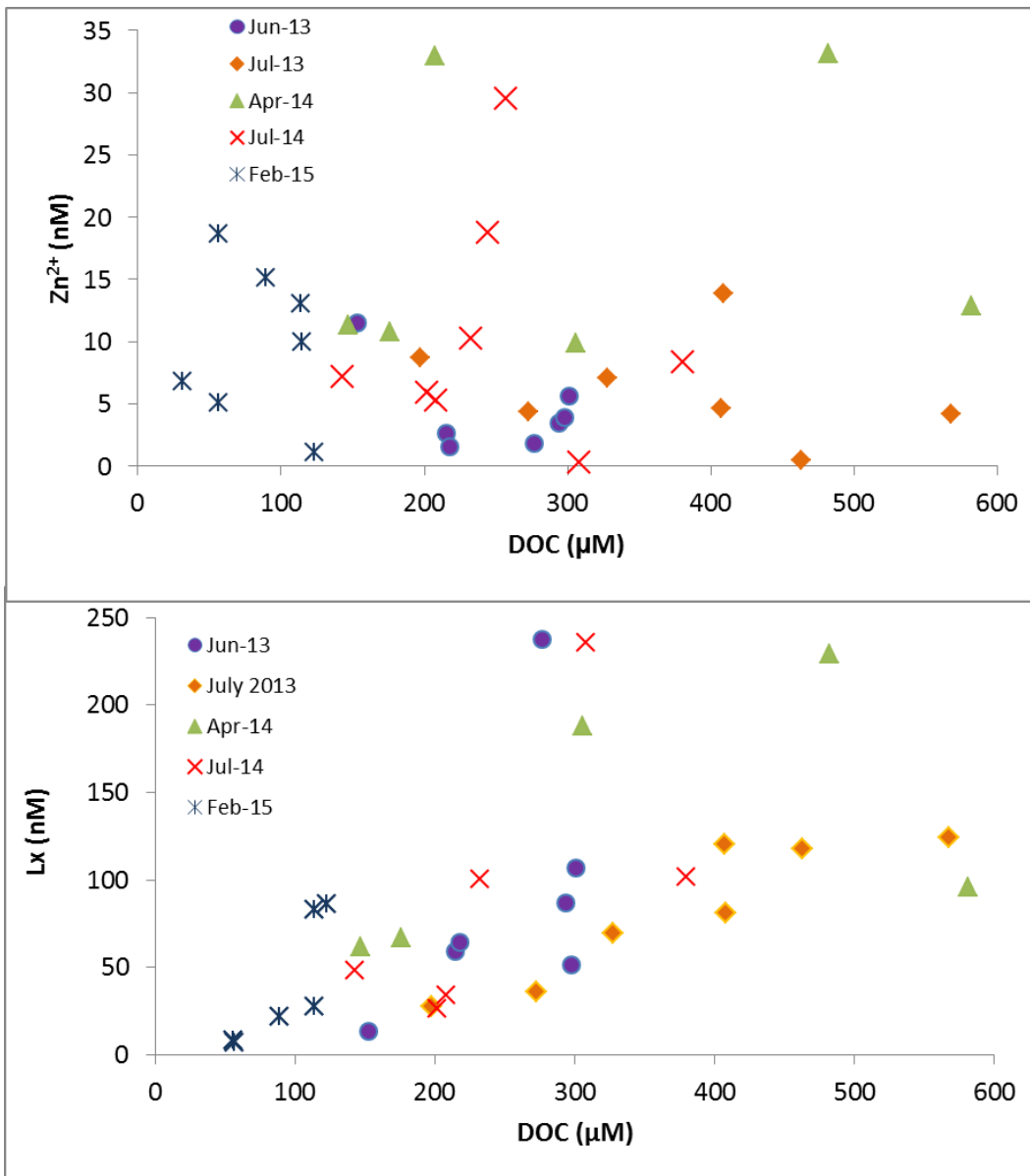
### 388 **3.4 Relationships between free Zn ion and DOC**

389 The results of  $\text{VM}_{\text{Tamar}}$  calculations show that it is possible to use VM to predict the  $[\text{Zn}^{2+}]$  to  
390 within an order of magnitude when details for site-specific complexation parameters (ligand  
391 concentrations and conditional stability constants of metal-ligand complexes) are entered into  
392 the model. This provides a certain degree of confidence in the agreement between the  
393 speciation programme outputs for Zn and measured ligand parameters that can be factored  
394 into a safety margin with respect to setting EQSs. However, the model outputs for predicted  
395 free metal ion concentration based on inputs of DOC concentrations alone gave a poorer  
396 prediction of the free ion concentration, and therefore the most potentially bioavailable and  
397 toxic metal fraction. The possible reasons for this have been explored further below.

398 DOC concentrations of 30 to 500  $\mu\text{M C}$  in the samples were consistent with those observed  
399 previously in the Tamar.<sup>39</sup> In comparison, zinc complexation capacities for the samples were  
400 in the region of 10 to 500 nM, typically three orders of magnitude lower (Figure 3). This  
401 demonstrates the complexity and challenges associated with attempting to predict the  
402 complexing ligands based on such a gross measure of what is a group of compounds with  
403 wide variability in physico-chemical characteristics and sources.

404 Plotting  $[Zn^{2+}]$  versus DOC (Figure 6) shows no specific trends either for the whole dataset or  
405 individual sampling occasions. A similar conclusion has been drawn for  $Cu^{2+}$  for estuarine  
406 samples.<sup>20</sup> The lack of data for Zn speciation in saline waters means there are no data to  
407 corroborate these findings, which in itself was a key incentive to undertake this research.  
408 Plotting Zn complexation capacity (Lx) against DOC showed a weak positive correlation, but  
409 at higher DOC concentrations the data scatter became pronounced. The only firm conclusion  
410 which may therefore be drawn is that at low DOC concentrations, complexation capacity is  
411 low, with complexation capacity likely to be higher where DOC concentrations exceed 300  $\mu M$ .  
412 For the purposes of predicting  $[Zn^{2+}]$ , there is no obvious relationship that could be applied.  
413 The fact that the complexation, and therefore  $[Zn^{2+}]$ , is controlled by both the ligand  
414 concentration and its strength, explains the lack of comparability between the plots of  $[Zn^{2+}]$   
415 and DOC, and  $[Zn^{2+}]$  and complexation capacity.

416



417

418 **Figure 6. [Zn<sup>2+</sup>] (top) and Zn complexation capacity (Lx, bottom) versus DOC for the**  
 419 **Tamar estuary samples.**

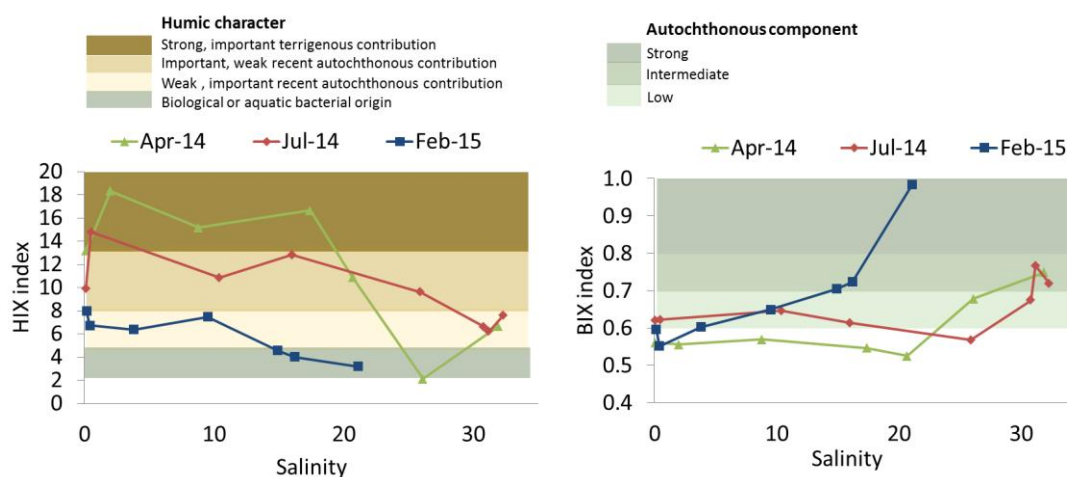
420

### 421 3.5 Further DOC characterization

422 There are techniques available to better characterize dissolved organic matter using UV and  
 423 fluorimetric methods. 3-D fluorimetry allows a semi-quantitative assessment of the  
 424 characteristics of compounds making up the DOC present in a sample. The ratios of  
 425 observed fluorescence peaks can be used to categorise the organic carbon as humic  
 426 and fulvic, terrestrial or *in situ* generated material using the humification (HIX) and  
 427 biological (BIX) indices (S2.4). HIX ratios (Ex260-Em320)/(Ex260-Em460) <4 suggest  
 428 biological or aquatic bacterial origin, while increasing humic character up to ratios >16  
 429 show progressively stronger humic character (Figure 7).<sup>12</sup> For BIX (Ex310-

430 Em380)/(Ex310-Em430) it has been observed that high ratios (0.8–1.0) corresponded  
 431 to a predominantly autochthonous origin of DOC from recent aquatic and bacterial  
 432 activity freshly released into water.<sup>13</sup>

433 In samples from the Tamar surveys, HIX values generally decreased towards the sea  
 434 water end member (Figure 7, no data for July 2013). Important humic character was  
 435 indicated for the fresh water endmember (HIX > 10), while DOC generated by *in situ*  
 436 biological processes increased in importance towards the sea water end member (BIX >  
 437 0.7). It is likely that the DOC in the lower estuary was at least partially derived from  
 438 phytoplanktonic activity and/or sewage effluents from works present in the lower  
 439 estuary.



440

441

442 **Figure 7. The humification (HIX) and biological (BIX) indices for each seasonal transect**  
 443 **against salinity (no data was available for 2013).**

444

445 Upper estuary and riverine HIX indices were > 10 during three surveys, supporting the  
 446 hypothesis that the DOC was of mainly terrestrial origin, comprising mostly humic and  
 447 fulvic acids. The BIX index corroborated this, with values increasing towards the sea  
 448 water end member, demonstrating the autochthonous origin of the DOC present.

449 A plot of [Lx] against HIX and BIX shows weak positive and negative correlations,  
 450 respectively (Figure S5). Highest HIX values were associated with higher complexation  
 451 capacities, which suggests a significant affinity of Zn for humic and fulvic acids,<sup>40</sup> which  
 452 dominate the lower salinity regions in the upper estuary (Figure S5). Any correlation  
 453 with BIX indices is hampered by the relatively small range of BIX (typically 0.6 to 0.8)

454 in the Tamar Estuary. Based on this dataset, it suggests that neither of these indices  
455 would be sufficiently robust to improve greatly on the existing use of DOC concentration  
456 as a surrogate for Zn complexation characterization.

457 This result corroborates the findings that there is no apparent simply defined relationship  
458 between DOC concentration and  $[Zn^{2+}]$  and lends support to the argument that assuming a  
459 fixed “active” portion (50 %) of DOC in a model such as WHAM or VM may be inappropriate,  
460 at least in regards to  $[Zn^{2+}]$ . VM has been reported to consistently underestimate free Cu ion<sup>41</sup>  
461 by between 2 and 5 orders of magnitude in comparison to measured values (in the range  $10^{-12}$   
462  $- 10^{-14}$  M) which are potentially controlled via multiple ligand sources at varying  
463 concentrations as discussed earlier. A key issue is that whether optimized ratios of measured  
464 DOC to ‘active’ FA fall within previously observed ranges. If not then this might suggest a role  
465 for ligands stronger than those humics can provide. The modeling using default data  
466 consistently overestimates  $[Zn^{2+}]$ , which suggests that there may be strong specific ligands in  
467 the estuary.

468 In the case of the over-prediction of  $[Zn^{2+}]$  by VM, the effect of synthetic ligands present in  
469 sewage effluent discharged to natural waters, such as ethylenediaminetetraacetic acid (EDTA)  
470 is not accounted for in the model, were discounted as a possible cause. Stockdale et al.,<sup>1</sup>  
471 tested EDTA concentrations within the WHAM/Model VII as low as  $5 \times 10^{-8}$  M and there was  
472 a small but noticeable effect for Zn (no effect for Cd and a greater effect for other metals) at  
473 this low concentration. Although concentrations of 0.1 and 1  $\mu$ M EDTA caused a considerable  
474 reduction (63% and 96% respectively) in calculated  $[Zn^{2+}]$ , these effective EDTA  
475 concentrations are unlikely to exist in the Tamar estuary. Although not quantified in this study,  
476 significant dilution of EDTA from the likely predominant sources (Ernesettle, Central, Marsh  
477 Mills and Camels Head WwTW, serving a combined population of 290,000) near the mouth of  
478 the estuary is probable. If the sewage effluent discharge in the Tamar is estimated at 72 million  
479 litres a day,<sup>42</sup> setting this against an average river discharge of 2333 million litres a day<sup>43</sup>  
480 equates to a 32 times dilution on river flow alone, without allowing for seawater flushing of the  
481 estuary. Based on recently published median effluent EDTA concentrations of 0.44  $\mu$ M<sup>44</sup> such  
482 a dilution would reduce the EDTA concentration to well below the effective concentration of  
483 ligands observed in this study. This does not exclude the possibility there are other  
484 anthropogenic synthetic ligands present within the estuary unaccounted for, but given the  
485 strength and typically high concentrations of EDTA present in effluents which have been  
486 discounted above, it seems unlikely more powerful ligands may be present at sufficient  
487 concentrations to impact on the Zn speciation.

488 Overall, the data presented here for Zn speciation along transects of the Tamar estuary were  
489 carried out to investigate the influence of dissolved organic ligands over the course of a  
490 calendar year, with the aim of attempting to model Zn speciation based on a limited dataset.  
491 It was not possible to attribute observed trends in metal speciation to any single measurable  
492 physico-chemical parameter, which was unsurprising as the complexity of the estuarine  
493 environment means observations are the result of a combination of many factors which are  
494 subject to constant change. In cases where rainfall has been abnormally high (e.g. February  
495 2015 survey), the expected trends and concentrations of constituents (e.g. DOC) can change  
496 dramatically, and therefore, mixing and physico-chemical parameters, such as turbidity, are  
497 likely the more important controls on speciation, rather than time of year.

498 Ligand abundance and excess, type, and binding strength appear to be important factors in  
499 controlling the proportion of complexed metal. Although these parameters are measurable  
500 with laboratory instrumentation there is no simple relationship between these factors and  
501 easily determined variables such as salinity, DOC or even further characterization of the DOC  
502 present using 3-D fluorimetry.

503 Modeling using VM generated reasonably accurate estimates of  $Zn^{2+}$ , provided site specific  
504 values for ligand strength and concentration were entered. Inputting DOC concentration and  
505 allowing the model's in-built algorithm to estimate complexation capacity generated over-  
506 estimates of  $Zn^{2+}$ , particularly at low salinities, where default fulvic acid log K assumptions  
507 appear to under-estimate complexation. A similar trend was observed for the WHAM VII model  
508 with much improved agreement between predicted and observed free metal ion at higher  
509 salinities, and uncertainties of measured values exceeding those of predictions.

510 Although models generating over-estimates of the more toxic Zn species is a conservative  
511 approach to risk assessments, to develop BLMs for estuarine waters it is necessary to be able  
512 to accurately predict free metal ion concentrations. The Tamar data presented here for Zn  
513 speciation (which are scarce in comparison with Cu speciation data) for the first time provide  
514 vital metal-ligand complexing strengths and ligand concentrations detected at various  
515 competitive ligand strengths across full salinity ranges which may be used for future modeling  
516 and regulatory purposes.

## 517 **Acknowledgements**

518 This work was co-funded by the European Copper Institute, International Zinc Association and  
519 Plymouth University. With thanks to the Plymouth University laboratory technical staff,  
520 constructive comments by funding partners, David Rushby for skippering the boat along the

521 Tamar, Dr. Aga Kosinska and David Deruytter for assistance in the laboratory and Dr. Alan  
522 Tappin for DOC analysis.

## 523 Supporting Information

524 The following material is supplied in the Supporting Information:

- 525 • Sample collection and storage
- 526 • Detailed analytical methodology
- 527 • Visual Minteq modeling
- 528 • WHAM modeling
- 529 • Additional figures and tables

530

## 531 References

532 1. Stockdale, A.; Tipping, E.; Lofts, S. Dissolved trace metal speciation in estuarine  
533 and coastal waters: comparison of WHAM/Model VII predictions with analytical results.  
534 *Environ. Toxicol. Chem.* **2015**, *34* (1), 53-63.

535 2. Pearson H.; Comber S., Braungardt C.; Worsfold P.; Galceran J.; Companys E.;  
536 Puy J. Absence of Gradients and Nernstian Equilibrium Stripping (AGNES) for the  
537 determination of [Zn<sup>2+</sup>] in estuarine waters. *Analyt. Chim. Acta.* **2016**, *912*, 32-40.  
538 <http://www.ncbi.nlm.nih.gov/pubmed/26920770>.

539 3. USEPA. 2007. Aquatic life ambient freshwater quality criteria - copper, 2007  
540 revision. U.S. Environmental Protection Agency, EPA-822-R-07-001 (March 2, 2007),  
541 Washington, DC. **2007**. <http://www.epa.gov/waterscience/criteria/copper/>

542 4. Maycock, D.; Merrington G.; Peters, A. *Proposed EQS for Water Framework*  
543 *Directive Annex VIII substances: copper (saltwater) (For consultation)*; Edinburgh, 2012.

544 5. Brix, K.V.; DeForest D.K.; Tear L.M.; Grosell M.; Adams W.J. Use of multiple linear  
545 regression models for setting water quality criteria for copper: A complementary approach to  
546 the Biotic Ligand Model. *Environ. Sci. Technol.* **2017**, *51* (9), 5182–5192;  
547 <https://doi.org/10.1021/acs.est.6b05533>.

548  
549 6. Brix, K.V.; DeForest D.K.; Adams W.J. Multiple Linear Regression (MLR) Models for  
550 Predicting Chronic Aluminum Toxicity to Freshwater Aquatic Organisms and Developing  
551 Water Quality Guidelines. *Environ. Toxicol. Chem.* **2018**, *37* (1), 80-90;  
552 <https://doi.org/10.1002/etc.3922>.

553 7. USEPA United States Environmental Protection Agency, National Recommended  
554 Water Quality Criteria - Aquatic Life Criteria Table; [https://www.epa.gov/wqc/national-](https://www.epa.gov/wqc/national-recommended-water-quality-criteria-aquatic-life-criteria-table)  
555 [recommended-water-quality-criteria-aquatic-life-criteria-table](https://www.epa.gov/wqc/national-recommended-water-quality-criteria-aquatic-life-criteria-table), **2016**.

556 8. Tipping, E. WHAM – a chemical equilibrium model and computer code for waters,  
557 sediments and soils incorporating a discrete-site electrostatic model of ion-binding by humic  
558 substances. *Comput. Geosci.* **1994**, *20* (6), 973–1023.

559 9. Tipping, E.; Lofts, S.; Sonke, J. Humic Ion-Binding Model VII: A revised  
560 parameterisation of cation-binding by humic substances. *Environ. Chem.* **2011**, *8* (3), 225-235.

- 561 10. Hudson, R. J. M., Trace metal uptake, natural organic matter, and the free-ion  
562 model. *J. Phycology* **2005**, 41, (1), 1-4.
- 563 11. Ytreberg E.; Karlsson J.; Eklund B.; Ndungu K. Effect of organic complexation on  
564 copper accumulation and toxicity to the estuarine red macroalga *Ceramium tenuicorne*: a test  
565 of the free ion activity model. *Environ. Sci Technol.* **2011**, 45 (7) 3145-53.
- 566 12. Zsolnay, Á. Dissolved organic matter: artefacts, definitions, and functions.  
567 *Geoderma*, **2003**, 113, (3–4), 187-209.
- 568 13. Huguet, A.; Vacher, L.; Relexans, S.; Saubusse, S.; Froidefond, J. M.; Parlanti, E.,  
569 Properties of fluorescent dissolved organic matter in the Gironde Estuary. *Org. Geochem.*  
570 **2009**, 40, (6), 706-719.
- 571 14. Gustafsson P. Visual MINTEQ model 3.1, <http://VMINTEQ.lwr.kth.se/>. **2013**.
- 572 15. Langston, W. J.; Chesman, B. S.; Burt, G. R.; Hawkins, S. J.; Readman, J.; Worsfold,  
573 P., *Characterisation of the South West European Marine Sites. Plymouth Sound and Estuaries*  
574 *cSAC, SPA. Occasional Publications. Mar. Biol. Assoc. UK* (9), 2003.
- 575 16. Mighanetara, K.; Braungardt, C. B.; Rieuwerts, J. S.; Azizi, F. Contaminant fluxes from  
576 point and diffuse sources from abandoned mines in the River Tamar catchment, *UK. J.*  
577 *Geochem. Explor.* **2009**, 100, (2–3), 116-124.
- 578 17. Rule, K. L.; Comber, S. D. W.; Ross, D.; Thornton, A.; Makropoulos, C. K.; Rautiu, R.  
579 Sources of priority substances entering an urban wastewater catchment—trace organic  
580 chemicals. *Chemosphere.* **2006**, 63, (4), 581-591.
- 581 18. Constantino, C. The effect of sewage effluent on trace metal speciation: Implications  
582 for the biotic ligand model approach. Brunel University, Uxbridge, **2012**.
- 583 19. Trigueros, J. M.; Orive, E., Tidally driven distribution of phytoplankton blooms in a  
584 shallow, macrotidal estuary. *J. Plank. Res.* **2000**, 22, (5), 969-986.
- 585 20. Pearson H.; Comber S.; Braungardt C.; Worsfold P. Predicting copper speciation and  
586 potential bioavailability in estuarine waters – Is dissolved organic carbon a good proxy for the  
587 presence of organic ligands? *Environ. Sci. Technol.* **2017**, 51,4, 2206-2216; DOI:  
588 10.1021/acs.est.6b05510.
- 589 21. Ružić, I. Theoretical aspects of the direct titration of natural waters and its information  
590 yield for trace metal speciation. *Analyt. Chim. Acta.* **1982**, 140, (1), 99-113.
- 591 22. van den Berg, C.M.G. *Determination of the zinc complexing capacity in seawater by*  
592 *cathodic stripping voltammetry of zinc—APDC complex ions.* *Mar. Chem.* **1985**. 16 (2), 121-  
593 130.
- 594 23. Badr, E.S.A.; Achterberg, E.P.; Tappin, A.D.; Hill, S.J.; Braungardt, C.B.  
595 Determination of dissolved organic nitrogen in natural waters using high-temperature  
596 catalytic oxidation. *TrAC Trends in Anal. Chem.* **2003**, 22, (11), 819-827.
- 597 24. Malcolm R.L.; McCarty P. Limitations in the use of commercial humic acids in water  
598 and soil research. *Environ. Sci. Technol.* **2006**, 20 (9), 904-911.
- 599 25. van den Berg, C. M. G.; Kramer, J. R., Determination of complexing capacities of  
600 ligands in natural waters and conditional stability constants of the copper complexes by means  
601 of manganese dioxide. *Anal. Chim. Acta* **1979**, 106, (1), 113-120.
- 602 26. Stumm, W. Morgan, J.J. *Aquatic Chemistry*, 3<sup>rd</sup> edn, Wiley, New York, **1996**.
- 603 27. Pierrot, D.; Lewis, E.; Wallace.; D. W. R. MS Excel Program Developed for CO<sub>2</sub> System  
604 Calculations. Carbon Dioxide Information Analysis Center. Oak Ridge National Laboratory,  
605 U.S. Department of Energy, Oak Ridge, Tennessee., **2006**.

- 606 28. Mehrbach, C.; Culberson, C. H.; Hawley, J. E.; Pytkowicz, R. M. Measurement of  
607 the apparent dissociation constants of carbonic acid in seawater at atmospheric pressure.  
608 *Limnol. Oceanogr.* **1973**, 18 (6), 897–906.
- 609 29. Dickson, A. G. Standard potential of the reaction:  $\text{AgCl(s)} + 12\text{H}_2\text{(g)} = \text{Ag(s)} +$   
610  $\text{HCl(aq)}$ , and the standard acidity constant of the ion  $\text{HSO}_4^-$  in synthetic sea water from  
611 273.15 to 318.15 K. *J. Chem. Thermodyn.* **1990**, 22 (2), 113–127.
- 612 30. Dickson, A. G.; Millero, F. J. A comparison of the equilibrium constants for the  
613 dissociation of carbonic acid in seawater media. *Deep-Sea Res. A.* **1987**, 34 (10), 1733–1743.
- 614 31. Gledhill, M.; Achterberg, E. P.; Li, K.; Mohamed, K. N.; Rijkenberg, M. J. A.  
615 Influence of ocean acidification on the complexation of iron and copper by organic ligands in  
616 estuarine waters. *Mar. Chem.* **2015**, 177, 421-433.
- 617 32. Lofts, S.; Tipping, E. Assessing WHAM/Model VII against field measurements of  
618 free metal ion concentrations: model performance and the role of uncertainty in parameters  
619 and inputs. *Environ. Chem.* **2011**, 8, 501-516.
- 620 33. Millward, G.E.; Liu, Y.P. Modelling metal desorption kinetics in estuaries. *Sci Tot*  
621 *Environ.* **2003**, 314-316, 613-623.
- 622 34. van den Berg, C.M.G.; A.G.A. Merks A.G.A; Duursma E.K. Organic complexation  
623 and its control of the dissolved concentrations of copper and zinc in the Scheldt estuary. *Est.*  
624 *Coast. Shelf Sci.* **1987**, 24 (6), 785-797.
- 625 35. Miao, A.J.; Wang X.W.; Juneau P. Comparison of Cd, Cu, and Zn toxic effects on  
626 four marine phytoplankton by pulse-amplitude-modulated fluorometry. *Environ. Toxicol. Chem.*  
627 **2005**. 24 (10), 2603-2611.
- 628 36. Kozelka, P.B. and K.W. Bruland, Chemical speciation of dissolved Cu, Zn, Cd, Pb  
629 in Narragansett Bay, Rhode Island. *Mar. Chem.* **1998**. 60 (3), 267-282.
- 630 37. Bryan S.E.; Tipping E.; Hamilton-Taylor J. Comparison of measured and modelled  
631 copper binding by natural organic matter in freshwaters. *Comp. Biochem. Physiol. Pt.*  
632 *C: Toxicol. & Pharmacol.*, **2002**, 133, 37-49.
- 633 38. Tipping, E.; Lofts, S.; Stockdale, A. Metal speciation from stream to open ocean:  
634 modelling v. measurement *Environ. Chem.* **2016**, 13, 464–477.
- 635 39. Miller, A.E.J. Seasonal investigations of dissolved organic carbon dynamics in the  
636 Tamar Estuary, U.K. *Est. Coast. Shelf Sci.* **1999**, 49, 981-908.
- 637 40. van den Berg C.M.G., Buckley P.J.M., Qiang Huang Z. and Nimmo M. An  
638 electrochemical study of the speciation of copper, zinc and iron in two estuaries in England.  
639 *Est. Coast. Shelf Sci.*, 1986, 22,4:479-486.
- 640 41. Unsworth, E.R.; Zhang H.; Davison W. Use of diffusive gradients in thin films to  
641 measure cadmium speciation in solutions with synthetic and natural ligands: comparison with  
642 model predictions. *Environ. Sci. Technol.*, **2005**, p. 624.
- 643 42. Harrison, B., *The dissolution of zinc from sacrificial anodes into harbour waters and*  
644 *the associated impacts on designated areas within Plymouth Sound*, in *School of Geography*  
645 *Earth and Environmental Sciences*. 2015, Plymouth University: Plymouth. p. 123.
- 646 43. Tattersall, G.R.; Elliott A.J.; Lynn N.M. Suspended sediment concentrations in the  
647 Tamar estuary. *Est. Coast. Shelf Sci.* **2003**, 57 (4), 679-688.
- 648 44. Gardner, M.; Comber, S.; Scrimshaw, M. D.; Cartmell, E.; Lester, J.; Ellor, B., The  
649 significance of hazardous chemicals in wastewater treatment works effluents. *Sci. Tot. Environ.*  
650 **2012**, 43, 363-372.

